International Journal of Bifurcation and Chaos, Vol. 28, No. 7 (2018) 1850089 (17 pages)

DOI: 10.1142/S021812741850089X

Turing Instability and Hopf Bifurcation in a Modified Leslie–Gower Predator–Prey Model with Cross-Diffusion

Walid Abid
University of Tunis El Manar,
National Engineering School of Tunis,
Laboratory of Engineering Mathematics EPT,
BP 743, La Marsa 2078, Tunisia
abidwalid007@yahoo.fr

R. Yafia*
Université Ibn Zohr,
BP 32/S, CP 80000 Agadir, Morocco
yafia1@yahoo.fr

M. A. Aziz-Alaoui
LMAH, FR-CNRS-3335,
Université du Havre Normandie, 25 Rue Ph. Lebon,
BP 540, 76058 Le Havre Cedex, (Normandie) France
aziz.alaoui@univ-lehavre.fr

Ahmed Aghriche
Université Ibn Zohr,
BP 32/S, CP 80000 Agadir, Morocco
aghriche87@gmail.com

Received March 31, 2018

This paper is concerned with some mathematical analysis and numerical aspects of a reaction–diffusion system with cross-diffusion. This system models a modified version of Leslie–Gower functional response as well as that of the Holling-type II. Our aim is to investigate theoretically and numerically the asymptotic behavior of the interior equilibrium of the model. The conditions of boundedness, existence of a positively invariant set are proved. Criteria for local stability/instability and global stability are obtained. By using the bifurcation theory, the conditions of Hopf and Turing bifurcation critical lines in a spatial domain are proved. Finally, we carry out some numerical simulations in order to support our theoretical results and to interpret how biological processes affect spatiotemporal pattern formation which show that it is useful to use the predator–prey model to detect the spatial dynamics in the real life.

Keywords: Cross-diffusion; Hopf bifurcation; pattern formation; Turing instability.

*Author for correspondence

1. Introduction

In recent years, the dynamic interaction between prey and their predators has become and will continue to be one of the dominant themes in the ecological sciences due to its universal existence and importance. The first model describing the dynamics of two interacting populations as a predator–prey system was developed independently by Alfred Lotka [Lotka, 1925] and Vito Volterra [Volterra, 1926]. It consists of two differential equations with a simple correspondence between prey consumption and predator production. The link between the dynamics of the two species is based on a linear functional response type, which represents the number of prey consumed per predator per unit of time, governed by the following differential equations

$$\begin{cases} \dot{u}(t) = u(t)(a - bv(t)), \\ \dot{v}(t) = v(t)(-c + fu(t)). \end{cases} \tag{1}$$

This model has the unavoidable limitations to describe many realistic phenomena in biological sciences. In order to well describe the real ecological interactions between the predator–prey species, many authors have suggested some improvements to the original model, such as considering different functional response types which is the function representing the prey consumption per unit time: Holling-types I–III [Holling, 1959], Beddington–DeAngelis type [DeAngelis *et al.*, 1975] and ratio-dependence type [Arditi & Ginzburg, 1989], etc. For more details, we refer to [Daher Okiye & Aziz-Alaoui, 2002; Hsu & Hwang, 1999; Li & Xiao, 2007; Liang & Pan, 2007].

One of the important improvements in the predator–prey interaction is the proposal by Turing [1952] — the striking idea of "diffusion-driven instability" in reaction–diffusion systems. These systems are often employed to investigate chemical and biological pattern formations and have received much attention from scientists [Camara & Aziz-Alaoui, 2008a; Wang, 2008; Yafia & Aziz-Alaoui, 2013; Abid *et al.*, 2015b; Camara & Aziz-Alaoui, 2008b].

In the last decades, one of the important predator–prey models is Leslie–Gower model [Leslie, 1948], which has been extensively studied by many authors [Nindjin *et al.*, 2006; Camara & Aziz-Alaoui, 2008a; Aziz-Alaoui & Daher Okiye, 2003; Daher Okiye & Aziz-Alaoui, 2002; Abid *et al.*, 2015c]. Recently, a modified version of Leslie–Gower predator–prey model with Holling-type II functional response was introduced by Aziz-Alaoui *et al.* (see [Camara & Aziz-Alaoui, 2008a; Aziz-Alaoui & Daher Okiye, 2003; Abid *et al.*, 2015a]) and the corresponding reaction–diffusion model is as follows:

$$\begin{cases} \dfrac{\partial U(X,Y,T)}{\partial T} = d_1 \Delta U(X,Y,T) + \left(a_1 - b_1 U(X,Y,T) - \dfrac{c_1 V(X,Y,T)}{U(X,Y,T) + K_1}\right) U(X,Y,T), \\ \dfrac{\partial V(X,Y,T)}{\partial T} = d_2 \Delta V(X,Y,T) + \left(a_2 - \dfrac{c_2 V(X,Y,T)}{U(X,Y,T) + K_2}\right) V(X,Y,T), \end{cases} \tag{2}$$

with initial conditions $U(0) > 0$ and $V(0) > 0$.

This two-species food chain model describes a prey population U which serves as food for a predator V.

The functions $U(X,Y,T)$ and $V(X,Y,T)$ are densities of the prey and predator, respectively at time T and position (X,Y), $\Delta = \frac{\partial^2}{\partial X^2} + \frac{\partial^2}{\partial Y^2}$ is the usual Laplacian operator in two-dimensional space. The model parameters are positive constants.

This system was studied by Camara *et al.* [Camara & Aziz-Alaoui, 2008a], they showed the dynamics and the asymptotic behavior of the system and prove the occurrence of Turing and Hopf bifurcation.

In [Yafia & Aziz-Alaoui, 2013], the authors showed the existence of the periodic traveling waves via Hopf bifurcation theorem by considering the diffusion as a parameter of bifurcation.

In recent years, several researches have been devoted to the studies of the dynamic relationship between predators and their prey, see [Nindjin *et al.*, 2006; Camara & Aziz-Alaoui, 2008a; Aziz-Alaoui & Daher Okiye, 2003; Daher Okiye & Aziz-Alaoui, 2002; Dancer, 1984; Hu & Li, 2012].

In nature, predator chases the prey (prey attracts predators), and prey tries to escape from the predator (predator repels prey). Such differential dispersal interactions can be modeled by the inclusion of so-called cross-diffusion [Kerner, 1959; Rosen, 1977] terms in reaction–diffusion models. Cross-diffusion means the diffusive movement is determined by the density gradient of another species population.

The first reaction–diffusion system with cross-diffusion was proposed by Shigesada *et al.* [1979] to investigate the habitat segregation phenomena between two population species. Since then, a lot of papers have been devoted to this field. In general, several researchers [Freedman, 1987; Okubo, 1980; Chattopadhyay *et al.*, 1996] have investigated the dynamics of interacting population with self- and cross-diffusion.

Cross-diffusion enunciates that the population fluxes of one species are derived from the presence of the other species. The value of the cross-diffusion coefficient can be positive, negative or zero. The term positive cross-diffusion coefficient leads to the movement of the species in the direction of lower concentration of another species. The term negative cross-diffusion coefficient results in one species diffusing in the direction of advanced concentration of another species.

A number of works have focused on the studies of the dynamic relationship between predators and their prey with cross-diffusion [Dubey & Das, 2001; Shi *et al.*, 2011; Zhou & Kim, 2013; Kuto, 2004; Kuto & Yamada, 2005; Xu, 2008].

In [Li, 2013], the authors studied the global asymptotic stability of the constant positive steady state on a cross-diffusion predator–prey system with Holling-type II functional response.

Lian and Huang [2014] studied the pattern formation of a cross-diffusion predator–prey system with the Allee effect. In addition, Sun and Wang [Sun *et al.*, 2012; Wang *et al.*, 2011] analyzed the spatial pattern formation of a predator–prey model with cross-diffusion.

In [Wen, 2013; Hu & Li, 2012], the authors studied the dynamics and the asymptotic behavior of the system and proved the occurrence of Turing and Hopf instability for a cross-diffusion predator–prey system with Holling-type II functional response.

The main aim of this paper is to investigate the dynamical complexity of the proposed model by Camara and Aziz-Alaoui [2008b] by introducing the term of cross-diffusion, in order to have the effect of cross-diffusion on the behavior of the solution. We prove the local and global stability of the positive steady state and show how cross-diffusion destabilizes stable equilibrium and is responsible for the initiation of spatial patterns. Our theoretical results are illustrated by numerical simulations.

The organization of the remaining part of the paper is as follows. In Sec. 2, we present the mathematical model, the existence and stability of the steady states of the model is proved. In Sec. 3, we derive the mathematical expressions for the Hopf and Turing bifurcation critical lines. In Sec. 4, we present the result of pattern formation via numerical simulation. In the end, we give some conclusions and discussions.

2. The Mathematical Model and Stability Analysis

Consider the predator–prey model (2) with

$$\begin{cases} \dfrac{\partial U(T,X,Y)}{\partial T} = D_1\Delta U(T,X,Y) + D_2\Delta V(T,X,Y) \\ \qquad\qquad + \left(a_1 - b_1 U(T,X,Y) - \dfrac{c_1 V(T,X,Y)}{U(T,X,Y)+K_1}\right) U(T,X,Y), \quad (X,Y)\in\Omega, \\ \dfrac{\partial V(T,X,Y)}{\partial T} = D_3\Delta U(T,X,Y) + D_4\Delta V(T,X,Y) \\ \qquad\qquad + \left(a_2 - \dfrac{c_2 V(T,X,Y)}{U(T,X,Y)+K_2}\right) V(T,X,Y), \quad (X,Y)\in\Omega, \end{cases} \tag{3}$$

where $\Omega \subset \mathbb{R}^n$ is a bounded domain with smooth boundary $\partial\Omega$, a_1 the growth rate of prey U, a_2 describes the growth rate of predators V, b_1 measures the strength of competition among individuals of species U, c_1 is the maximum value of the per capita reduction of U due to V, c_2 has a similar meaning to c_1, K_1 measures the extent to which the environment provides protection to prey U, K_2 has a similar meaning to K_1 relatively to the predator V, d_1 and d_4 are self-diffusion coefficients of prey and predator, d_2 and d_3 are the cross-diffusion coefficients of prey and predator respectively.

In order to minimize the number of parameters involved in the model, it is extremely useful to write the system without diffusion in nondimensionalized form. Thus we take

$$t = a_1 T, \quad u = \frac{b_1}{a_1}U, \quad v = \frac{c_2 b_1}{a_1 a_2}V, \quad a = \frac{a_2 c_1}{a_1 c_2}, \quad b = \frac{a_2}{a_1}, \quad e_1 = \frac{b_1 k_1}{a_1},$$

$$e_2 = \frac{b_1 k_2}{a_1}, \quad x = \frac{X}{L}, \quad y = \frac{Y}{L}, \quad d_1 = \frac{D_1}{a_1 L^2}, \quad d_2 = \frac{a_2 D_2}{c_2 a_1 L^2},$$

$$d_3 = \frac{c_2 D_3}{a_1 a_2 L^2} \quad \text{and} \quad d_4 = \frac{D_4}{a_1 L^2} \quad (L \text{ being the characteristic length}).$$

The spatiotemporal predator–prey model with cross-diffusion is given by

$$\begin{cases} \dfrac{\partial u(t,x,y)}{\partial t} = d_1 \Delta u(t,x,y) + d_2 \Delta v(t,x,y) + u(t,x,y)(1 - u(t,x,y)) \\ \qquad\qquad - \dfrac{av(t,x,y)}{u(t,x,y)+e_1} u(t,x,y), & (x,y) \in \Omega, \\ \dfrac{\partial v(t,x,y)}{\partial t} = d_3 \Delta u(t,x,y) + d_4 \Delta v(t,x,y) + b\left(1 - \dfrac{v(t,x,y)}{u(t,x,y)+e_2}\right) v(t,x,y), & (x,y) \in \Omega, \\ u(0,x,y) = u_0(x,y) > 0, \quad v(0,x,y) = v_0(x,y) > 0, & (x,y) \in \Omega, \\ \dfrac{\partial u}{\partial \eta} = \dfrac{\partial v}{\partial \eta} = 0, & (x,y) \in \partial\Omega. \end{cases} \tag{4}$$

Here we assume that the two populations of prey and predator are diffused in a bounded spatial domain $\Omega = [0, l_x] \times [0, l_y]$, l_x and l_y denote the sizes of the system in the directions of x and y, respectively, where η is the outward unit normal vector on $\partial\Omega$.

Next, we prove the existence of positive solutions and local and global stabilities of system (3).

2.1. *Existence of positive solutions*

In this section, we study the existence and nonexistence of positive equilibrium of the following elliptic system

$$\begin{cases} -\Delta[d_1 U + d_2 V] = \left(a_1 - b_1 U - \dfrac{c_1 V}{U + K_1}\right) U, \\ \qquad\qquad (X,Y) \in \Omega, \\ -\Delta[d_3 U + d_4 V] = \left(a_2 - \dfrac{c_2 V}{U + K_2}\right) V, \\ \qquad\qquad (X,Y) \in \Omega, \\ \dfrac{\partial u}{\partial \eta} = \dfrac{\partial v}{\partial \eta} = 0, \quad (X,Y) \in \partial\Omega. \end{cases} \tag{5}$$

$\Omega \subset \mathbb{R}^n$, we use $\|\cdot\|_B$ as the norm of Banach space B. For each $z \in C(\overline{\Omega})$, let $\lambda_1(z)$ be the principle eigenvalue of the following spectral problem.

$$\begin{cases} -\Delta U + z(X,Y)U = \lambda U, & (X,Y) \in \Omega, \\ \dfrac{\partial U}{\partial \eta} = 0, & (X,Y) \in \partial\Omega, \end{cases} \tag{6}$$

$\lambda_1(z)$ is given by the following variational characterization:

$$\lambda_1(z) = \inf_{\phi \in H_0^1, \|\phi\|_{L^2(\Omega)} = 1} \times \int_\Omega \int_\Omega (|\nabla\phi|^2 + z(X,Y)\phi^2)\, dX\, dY$$

and has some useful properties (for more details see [Zhou & Kim, 2013]).

Consider the following steady state problem for logistic equation with linear diffusion

$$\begin{cases} -\Delta U = U(\alpha - U), & (X,Y) \in \Omega, \\ U \geq 0, & (X,Y) \in \Omega, \\ \dfrac{\partial U}{\partial \eta} = 0, & (X,Y) \in \partial\Omega, \end{cases} \tag{7}$$

where α is a positive constant and $\Omega \subset \mathbb{R}^n$ is a bounded open set with smooth boundary $\partial\Omega$, then the following results are well known (see [Zhou & Kim, 2013]).

Theorem 1

(i) *If $\alpha \leq \lambda_1$, then system (7) has no nontrivial solutions.*
(ii) *If $\alpha > \lambda_1$, then there exists a unique positive solution $\theta_\alpha(X,Y)$ of (7) such that $\theta_\alpha(X,Y)$ is strictly increasing with respect to α and $0 < \theta_\alpha(X,Y) < \alpha$ for every $(X,Y) \in \Omega$.*

Introducing the functions

$$\begin{aligned} M_1 &= d_1U + d_2V, \\ M_2 &= d_3U + d_4V, \end{aligned} \tag{8}$$

there exists a one-to-one correspondence between $(U,V) \geq (0,0)$ and $(M_1,M_2) \geq (0,0)$. By using transformation defined in system (8), system (5) can be rewritten as follows:

$$\begin{cases} -\Delta M_1 = U\left(a_1 - b_1U - \dfrac{c_1V}{U+K_1}\right) = \dfrac{1}{d_1}(M_1 - d_2V)\left(a_1 - b_1U - \dfrac{c_1V}{U+K_1}\right) & (X,Y) \in \Omega, \\ -\Delta M_2 = V\left(a_2 - \dfrac{c_2V}{U+K_2}\right) = \dfrac{1}{d_4}(M_2 - d_3U)\left(a_2 - \dfrac{c_2V}{U+K_2}\right) & (X,Y) \in \Omega, \\ \dfrac{\partial u}{\partial \eta} = \dfrac{\partial v}{\partial \eta} = 0 & (X,Y) \in \partial\Omega. \end{cases} \tag{9}$$

The following result gives some *a priori* estimates for non-negative solutions of system (9).

Lemma 1. *Let (M_1,M_2) be a non-negative solution of system (9), then*

$$0 \leq U(X,Y) \leq \frac{M_1(X,Y)}{d_1} \leq T_1(a_1) := \frac{d_1a_1}{b_1}\left(d_1 + d_2\frac{(b_1k_1 + a_1)}{c_1}\right) \tag{10}$$

and

$$0 \leq V(X,Y) \leq \frac{M_2(X,Y)}{d_4} \leq T_2(a_1,a_2)$$

$$:= \begin{cases} 0 & \text{if } b = 0 \ \text{ or } \ K_2 = -T_1(a_1) \\ \dfrac{a_2}{c_2}(T_1(a_1) + K_2) + \dfrac{d_3}{d_4}T_1(a_1) & \text{if } \begin{cases} \dfrac{a_2}{c_2} > 0 \quad \text{and} \quad K_2 > -T_1(a_1) \\ \text{or} \\ \dfrac{a_2}{c_2} < 0 \quad \text{and} \quad -K_2 > T_1(a_1). \end{cases} \end{cases} \tag{11}$$

Proof. Firstly, we prove the estimates for U and M_1. Since $0 \leq U \leq \frac{M_1}{d_1}$ from (8), assume that $M_1(X,Y)$ attains its maximum at (X_0,Y_0). Since $M_1(X,Y)$ is non-negative in Ω and $\frac{\partial M_1}{\partial \eta}(X,Y) = 0$ on the boundary $\partial\Omega$, we may assume $(X_0,Y_0) \in \Omega$, thus

$$0 \leq -\Delta M_1 = U(X_0,Y_0)\left(a_1 - b_1U(X_0,Y_0) - \frac{c_1V(X_0,Y_0)}{U(X_0,Y_0) + K_1}\right). \tag{12}$$

If $U(X_0,Y_0) = V(X_0,Y_0) = 0$, then $M_1(X_0,Y_0) = 0$ by (8) and $M_1(X,Y) \equiv 0$ for $(X,Y) \in \overline{\Omega}$.

On the other hand, if $U(X_0,Y_0) > 0$, (12) implies

$$U(X_0,Y_0) \leq \frac{a_1}{b_1} \quad \text{and} \quad V(X_0,Y_0) \leq \frac{a_1(b_1k_1 + a_1)}{b_1c_1}.$$

Thus, by (8) we have

$$\begin{aligned} M_1(X,Y) &\le M_1(X_0,Y_0) \\ &= d_1U(X_0,Y_0)+d_2V(X_0,Y_0) \\ &\le d_1\frac{a_1}{b_1}+d_2\frac{a_1(b_1k_1+a_1)}{b_1c_1}, \\ &\qquad \forall (X,Y)\in\Omega. \end{aligned} \tag{13}$$

Now, by the same way for U, we will provide the estimate for V and M_2. $0 \le V \le \frac{M_2}{d_4}$ from (8) and by assuming that $M_2(X,Y)$ attains its maximum at (X_1,Y_1). Since $M_2(X,Y)$ is non-negative in Ω and $\frac{\partial M_2}{\partial\eta}(X,Y)=0$ on the boundary $\partial\Omega$, we may assume $(X_1,Y_1)\in\Omega$, thus

$$\begin{aligned} 0 &\le -\Delta M_2(X_1,Y_1) \\ &= V(X_1,Y_1)\left(a_2-\frac{c_2V(X_1,Y_1)}{U(X_1,Y_1)+K_2}\right). \end{aligned} \tag{14}$$

If $U(X_1,Y_1)=V(X_1,Y_1)=0$ then $M_2(X_1,Y_1)=0$ by (8) and $M_2(X,Y)\equiv 0$ or $(X,Y)\in\overline{\Omega}$, if $b=0$ or $K_2=-T_1(a_1)$ we affirm $V(X_1,Y_1)=0$. Indeed, if $V(X_1,Y_1)>0$ then (10) and (14) imply that

$$\begin{aligned} 0 &< V(X_1,Y_1) \\ &\le \frac{1}{c_2}(a_2U(X_1,Y_1)+a_2K_2) \\ &\le \frac{a_2}{c_2}(K_2+T_1(a_1)) \\ &= \frac{a_2}{c_2}(-T_1(a_1)+T_1(a_1))=0, \end{aligned} \tag{15}$$

which is a contradiction. Thus $V(X_1,Y_1)=0$ and (11) follows.

Finally, if $V(X_1,Y_1)>0$, $[\frac{a_2}{c_2}>0$ and $K_2>-T_1(a_1)]$ or $[\frac{a_2}{c_2}<0$ and $-K_2>T_1(a_1)]$ hold true, then (10) and (14) imply that

$$\begin{aligned} V(X_1,Y_1) &\le \frac{a_2}{c_2}(U(X_1,Y_1)+K_2) \\ &\le \frac{a_2}{c_2}(T_1(a_1)+K_2). \end{aligned}$$

Therefore

$$\begin{aligned} M_2(X,Y) &\le M_2(X_1,Y_1) \\ &= d_3U(X_1,Y_1)+d_4V(X_1,Y_1) \\ &\le d_3T_1(a_1)+d_4\frac{a_2}{c_2}(T_1(a_1)+K_2), \\ &\qquad \forall (X,Y)\in\Omega. \end{aligned} \tag{16}$$

The proof is completed. ■

Theorem 2. *System (9) has no positive solution if any one of the following conditions hold*:

(i) $a_1 \le \lambda_1$,
(ii) *for each* $a_1>0$, $b=0$ *or* $K_2=-T_1(a_1)$, (*where* $T_1(a_1)$ *is the constant defined in Lemma 1*).

Proof. Let (U,V) be a positive solution of (3). Then (M_1,M_2) defined in (8) is a positive solution of (9).

(i) Let $\Phi_1(X,Y)$ with $\|\Phi_1\|_{L^2(\Omega)}=1$ be the positive eigenfunction corresponding to λ_1.

Multiplying the first equation of (9) by Φ_1 and integrating it over Ω,

$$\begin{aligned} &\int_\Omega\int_\Omega -\Phi_1\Delta M_1 dXdY \\ &\quad = \int_\Omega\int_\Omega U\Phi_1\left(a_1-b_1U-\frac{c_1V}{U+K_1}\right)dXdY, \end{aligned}$$

since

$$\int_\Omega\int_\Omega -\Phi_1\Delta M_1 dXdY = \lambda_1\int_\Omega\int_\Omega U\Phi_1 dXdY,$$

therefore

$$\begin{aligned} &\int_\Omega\int_\Omega U\Phi_1\left(a_1-b_1U-\frac{c_1V}{U+K_1}\right)dXdY \\ &\quad = \lambda_1\int_\Omega\int_\Omega U\Phi_1 dXdY \end{aligned}$$

and

$$\begin{aligned} &\int_\Omega\int_\Omega U\Phi_1\left(a_1-b_1U-\frac{c_1V}{U+K_1}\right)dXdY \\ &\quad < a_1\int_\Omega\int_\Omega U\Phi_1 dXdY, \end{aligned}$$

$$\lambda_1\int_\Omega\int_\Omega U\Phi_1 dXdY < a_1\int_\Omega\int_\Omega U\Phi_1 dXdY,$$

$$(a_1-\lambda_1)\int_\Omega\int_\Omega U\Phi_1 dXdY > 0,$$

which implies that $a_1>\lambda_1$.

(ii) For each $a_1 > 0$, $b = 0$ or $K_2 = -T_1(a_1)$, then it follows from (11) that system (9) has no positive solution. ∎

2.2. *Equilibrium points and stability*

In this section, we recall some results on the asymptotic behavior of the system without diffusion

$$\begin{cases} \dfrac{du}{dt} = u(1-u) - \dfrac{av}{u+e_1}u \\ \dfrac{dv}{dt} = b\left(1 - \dfrac{v}{u+e_2}\right)v \\ u(0) > 0, \quad v(0) > 0, \end{cases} \tag{17}$$

we study some equilibria properties of system (17). These steady states are determined analytically by setting $\dot{u} = 0$, $\dot{v} = 0$. It is easy to verify that this system has three trivial boundary equilibria:

$$W_0 = (0,0), \quad W_1 = (1,0), \quad W_2 = (0, e_2)$$

and the nontrivial equilibrium is $W_3 = (u^*, v^*)$, where

$$\begin{cases} u^* = \dfrac{-(a - e_1 - 1) + \sqrt{(e_1 + 1 - a)^2 + 4(e_1 - ae_2)}}{2}, \\ v^* = u^* + e_2. \end{cases} \tag{18}$$

The Jacobian matrix associated with an equilibrium point (u, v) of (17):

$$G(u,v) = \begin{pmatrix} 1 - 2u - \dfrac{ae_1 v}{(u+e_1)^2} & -\dfrac{au}{u+e_1} \\ \dfrac{bv^2}{(u+e_2)^2} & b - \dfrac{2bv}{u+e_2} \end{pmatrix}.$$

Proposition 1

(i) *The equilibrium point $E_0 = (0,0)$ is unstable.*
(ii) *The equilibrium point $E_1 = (1,0)$ is unstable.*
(iii) *If $e_1 > ae_2$, then $E_2 = (0, e_2)$ is unstable and if $e_1 < ae_2$, then $E_2 = (0, e_2)$ is asymptotically stable.*

Now, we study the stability of the nontrivial equilibrium.

Proposition 2. *If the following conditions are satisfied*

$$2a \geq 1 \quad \textit{and}$$
$$0 \leq e_1 \leq -(a+1) + \sqrt{(a+1)^2 + 2a(1+2a) - 1}, \tag{19}$$

$$d_1 d_4 > d_2 d_3, \quad d_1 > 0, \quad d_2 > 0, \quad d_4 > 0 \quad \textit{and} \quad d_3 < 0, \tag{20}$$

then the equilibrium (u^*, v^*) is a stable node.

Proof. We consider the linearized problem of system (3):

$$\frac{\partial S}{\partial t} = DS + PS, \tag{21}$$

where

$$\mathbf{P} = \begin{pmatrix} 1 - 2u^* - \dfrac{e_1(1-u^*)}{u^*+e_1} & -\dfrac{au^*}{u^*+e_1} \\ b & -b \end{pmatrix} = \begin{pmatrix} h_1 & h_2 \\ h_3 & h_4 \end{pmatrix}$$

and

$$\mathbf{D} = \begin{pmatrix} d_1 & d_2 \\ d_3 & d_4 \end{pmatrix}, \quad S = \sum_{i=0}^{\infty} z_i(t)\Phi_i(x), \tag{22}$$

$z_i \in \mathbb{R}^2$, Φ_i is the eigenfunction of Δ defined on Ω, the problem associated with the operator $-\Delta$ with homogeneous Neumann boundary condition.

From (21) and (22), we obtain

$$\frac{dz_i}{dt} = (GP - \lambda_i D)z_i, \tag{23}$$

where λ_i are scalar such that $0 = \lambda_0 < \lambda_1 < \lambda_2 < \cdots$.

To show that the homogeneous equilibrium (u^*, v^*) is stable it suffices to show that each $z_i(t)$ decreases towards zero. This means that all the eigenvalues of $(GP - \lambda_i D)$ are of negative real part.

To determine the eigenvalues σ of $(GP - \lambda_i D)$ one needs to solve the following equation

$$\begin{aligned} \sigma^2 - \sigma(h_1 + h_4 - \lambda_i(d_1 + d_4)) + \lambda_i^2(d_1 d_4 - d_2 d_3) \\ - \lambda_i(d_1 h_4 + d_4 h_1 - d_2 h_3 - d_3 h_2) \\ + h_1 h_4 - h_2 h_3 = 0. \end{aligned}$$

The real part of each eigenvalue $(GP - \lambda_i D)$ is negative if

$$\begin{aligned} &h_1 + h_4 - \lambda_i(d_1 + d_4) < 0 \quad \text{and} \\ &\lambda_i^2(d_1 d_4 - d_2 d_3) - \lambda_i(d_1 h_4 + d_4 h_1 \\ &\quad - d_2 h_3 - d_3 h_2) + h_1 h_4 - h_2 h_3 > 0 \end{aligned} \tag{24}$$

or h_4 and h_2 are negative and $\lambda_i \geq 0$. Therefore the condition (24) is

$$h_1 \leq 0, \quad h_3 > 0, \quad d_1 d_4 > d_2 d_3, \quad d_1 > 0,$$
$$d_2 > 0, \quad d_4 > 0 \quad \text{and} \quad d_3 < 0.$$

So for $h_1 \leq 0$, we have

$$2u^* - 1 - e_1 \geq 0 \quad \text{and}$$
$$1 - e_1 - a + \sqrt{\Delta} - 1 + e_1 \geq 0.$$

Therefore

$$(a + e_1 - 1)^2 - 4(ae_1 - e_1) - a^2 \geq a \quad \text{and}$$
$$e_1^2 + 2e_1(a+1) - a(2 + 4e_2) + 1 \geq 0.$$

These two inequalities are satisfied under the assumptions of the proposal (2), therefore $1 - 2u^* - \frac{e_1(1-u^*)}{u^*+e_1} \leq 0$. Then (u^*, v^*) is stable. ■

Theorem 3. *If the following condition is satisfied*

$$1 \leq e_1 \leq e_2 \quad \textit{and}$$
$$d_1 > 0, \quad d_2 > 0, \quad d_3 > 0, \quad d_4 > 0 \tag{25}$$

then, the steady state (u^*, v^*) is globally asymptotically stable for Eq. (4).

Proof. The proof is based on a positive definite Lyapunov function. Let us denote by

$$l(u,v) = \int_{u^*}^{u} \frac{(\eta - u^*)(\eta + e_1)}{a\eta(\eta + e_2)} d\eta + \frac{u^* + e_2}{bv^*} \int_{v^*}^{v} \frac{\eta - v^*}{\eta} d\eta \tag{26}$$

and

$$\begin{aligned} L(u,v) &= \int_0^{l_y}\int_0^{l_x} l(u,v)\,dxdy \\ &= \int_0^{l_y}\int_0^{l_x}\left(\int_{u^*}^{u} \frac{(\eta - u^*)(\eta + e_1)}{a\eta(\eta + e_2)} d\eta \right. \\ &\quad \left. + \frac{u^* + e_2}{bv^*}\int_{v^*}^{v} \frac{\eta - v^*}{\eta} d\eta\right) dxdy, \end{aligned}$$

$L(u,v)$ is positive for all (u,v) in the positive quadrant, except for (u^*, v^*), for which $L(u^*, v^*) = 0$. Therefore we only have to show that $\frac{dL}{dt} < 0$.

The orbital derivative of L, along the flow of system (4) is

$$\begin{aligned} \frac{dL}{dt} &= \int_0^{l_y}\int_0^{l_x}\left(\frac{(u-u^*)(u+e_1)}{au(u+e_2)}\right)\left(d_1\Delta u + d_2\Delta v + u(1-u) - \frac{auv}{u+e_1}\right) dxdy \\ &\quad + \int_0^{l_y}\int_0^{l_x}\left(\frac{(u^*+e_2)(v-v^*)}{bvv^*}\right)\left(d_3\Delta u + d_4\Delta v + b\left(1 - \frac{v}{u+e_2}\right)v\right) dxdy \\ &= \int_0^{l_y}\int_0^{l_x}\left(\frac{(u-u^*)(u+e_1)}{au(u+e_2)}\right)\left(u(1-u) - \frac{auv}{u+e_1}\right) dxdy \\ &\quad + \int_0^{l_y}\int_0^{l_x}\left(\frac{(u^*+e_2)(v-v^*)}{bvv^*}\right)\left(b\left(1 - \frac{v}{u+e_2}\right)v\right) dxdy \\ &\quad + \int_0^{l_y}\int_0^{l_x}(d_1\Delta u + d_2\Delta v)\frac{(u-u^*)(u+e_1)}{au(u+e_2)} + (d_3\Delta u + d_4\Delta v)\frac{(u^*+e_2)(v-v^*)}{bvv^*} dxdy. \end{aligned} \tag{27}$$

Let us denote T_1 and T_2 as the terms of Eqs. (27). After simple algebraic computations, T_1 becomes

$$T_1 = -\int_0^{l_y}\int_0^{l_x}\left((u + u^* + e_1 - 1)\frac{u - u^*}{a(u+e_2)} + \frac{(v-v^*)^2}{u+e_2}\right) dxdy. \tag{28}$$

For T_2, by using the Green formula, we obtain

$$T_2 = -\int_0^{l_y}\int_0^{l_x}\left((d_1|\nabla u|^2 + d_2|\nabla v|^2)\frac{d}{du}\right.$$
$$\times\left(\frac{(u-u^*)(u+e_1)}{au(u+e_2)}\right) + \delta\frac{u^*+e_2}{bv^*}$$
$$\left.\times(d_3|\nabla u|^2 + d_4|\nabla v|^2)\frac{d}{dv}\left(\frac{v-v^*}{v}\right)\right)dxdy, \tag{29}$$

$$= -\int_0^{l_y}\int_0^{l_x}\left((d_1|\nabla u|^2 + d_2|\nabla v|^2)\right.$$
$$\times\left(\frac{(e_2-e_1+1+u^*)}{au(u+e_2)^2} + \frac{u^*e_1(2u+e_2)}{a(u^2+e_2u)^2}\right)$$
$$\left.+\,\delta\frac{u^*+e_2}{bv^*}(d_3|\nabla u|^2 + d_4|\nabla v|^2)\frac{v^*}{v^2}\right)dxdy. \tag{30}$$

From the final expressions of T_1 and T_2, we have $\frac{dL}{dt}(u,v) < 0$. Therefore, by LaSalle's theorem (u^*, v^*) is globally asymptotically stable. ■

3. Bifurcation Theory

In this section, we present the conditions of the occurrence of Hopf and Turing bifurcations and we study the stability behavior of the interior equilibrium point $W^* = (u^*, v^*)$.

Now to linearize the proposed diffusive mathematical model around (u^*, v^*) for space and time perturbation, we assume the following

$$u(\overrightarrow{g},t) = u^* + \overline{u}(\overrightarrow{g},t), \quad |\overline{u}(\overrightarrow{g},t)| \ll u^*,$$
$$v(\overrightarrow{g},t) = v^* + \overline{u}(\overrightarrow{g},t), \quad |\overline{v}(\overrightarrow{g},t)| \ll v^*$$

and

$$\begin{bmatrix}\overline{u}(\overrightarrow{g},t)\\ \overline{v}(\overrightarrow{g},t)\end{bmatrix} = \begin{bmatrix}\zeta_1\\ \zeta_2\end{bmatrix}e^{\lambda t + i\overrightarrow{k}\,\overrightarrow{g}}, \quad \overrightarrow{k} = (k_x, k_y),$$

where $\overrightarrow{g} = (x,y)$ is spatial vector; λ is the perturbed growth rate in time t; ζ_1, ζ_2 are the corresponding amplitudes and $k(=\sqrt{k_x^2+k_y^2})$ the wavenumber of the solution. Substituting the expression of perturbations into system (4), we obtain the following characteristic equation of the linearized system

$$\lambda^2 + H_k\lambda + E_k = 0, \tag{31}$$

with

$$\mathbf{N} = \begin{pmatrix}\lambda - h_1 + d_1k^2 & -h_2 + d_2k^2\\ -h_3 + d_3k^2 & \lambda - h_4 + d_4k^2\end{pmatrix}$$

and

$$H_k = (d_1+d_4)k^2 - (h_1+h_4), \tag{32}$$
$$E_k = (d_1d_4 - d_2d_3)k^4 - (d_1h_4 + d_4h_1 - d_2h_3 - d_3h_2)k^2 + h_1h_4 - h_2h_3. \tag{33}$$

Therefore, the eigenvalues are the roots of (31) and are given by

$$\lambda_k = \frac{-H_k \pm \sqrt{H_k^2 - 4E_k}}{2}. \tag{34}$$

The onset of Hopf instability corresponds to the case, when a pair of imaginary eigenvalues cross the real axis from the negative to the positive side and this situation occurs only when the diffusion vanishes. Mathematically speaking, the Hopf bifurcation occurs when

$$\mathrm{Im}(\lambda_k) \neq 0, \quad \mathrm{Re}(\lambda_k) = 0 \quad \text{at } k = 0. \tag{35}$$

From the roots dispersion given in Eq. (34), the critical value of Hopf bifurcation parameter b is

$$b_H = \frac{h_1 - b - \sqrt{(h_1-b)^2 + 4h_1b}}{2}$$
$$= 1 - 2u^* - \frac{e_1(1-u^*)}{u^*+e_1}. \tag{36}$$

If there is at least one positive root of (32), then system (4) will be unstable. By a simple analysis, we find that E_k is a quadratic polynomial with respect to k^2. Its extremum is a minimum at some k^2 (see [Sun *et al.*, 2009; Murray, 1993]). From E_k, elementary differentiation with respect to k^2 shows that

$$k_{\min}^2 = \frac{d_4h_1 + d_1h_4 - d_2h_3 - d_3h_2}{2(d_1d_4 - d_2d_3)}. \tag{37}$$

At this critical point, we have $E_k = 0$ when $k = k_c$ (see [Sun *et al.*, 2009]). For fixed kinetics parameters, this defines a critical cross-diffusion coefficient d_2 as the root of the following equation

$$(d_1h_4 + d_4h_1 - d_2h_3 - d_3h_2)^2 - 4(h_1h_4 - h_2h_3)(d_1d_4 - d_2d_3) = 0 \tag{38}$$

and we have

$$d_2 = \frac{-J \pm \sqrt{J^2 - 4RQ}}{2R}, \tag{39}$$

where

$$J = 2h_3d_3h_2 - 2h_3(d_1h_4 + d_4h_1) + 4d_3(h_1h_4 - h_2h_3),$$
$$Q = (d_1h_4 + d_4h_1)^2 + (d_3h_2)^2 - 2d_3h_2(d_1h_4 + d_4h_1) - 4d_1d_4(h_1h_4 - h_2h_3),$$
$$R = (h_3)^2.$$

Then, the critical wavenumber k_c is given by

$$k_c = \sqrt{\frac{h_1h_4 - h_2h_3}{d_1d_4 - d_2d_3}} = \sqrt{\frac{\det P}{\det D}}. \quad (40)$$

A general linear analysis (see [Jin *et al.*, 2008; Chung & Peacock-López, 2007]) shows that the necessary conditions for yielding Turing instability are given by

$$h_1 + h_4 < 0, \quad (41)$$
$$h_1h_4 - h_2h_3 > 0, \quad (42)$$
$$d_4h_1 + d_1h_4 - d_2h_3 - d_3h_2 > 0 \quad (43)$$

and

$$(d_4h_1 + d_1h_4 - d_2h_3 - d_3h_2)^2 - 4(h_1h_4 - h_2h_3)(d_1d_4 - d_2d_3) > 0. \quad (44)$$

Then, the Turing bifurcation occurs when

$$\mathrm{Im}(\lambda_k) = 0, \quad \mathrm{Re}(\lambda_k) = 0, \quad \text{at } k = k_c \neq 0 \quad (45)$$

and the wavenumber k_c is denoted the same as in (40). By direct calculation, it was assumed that $E_k = 0$ and $H_k = 0$, we obtain the following characteristic polynomial

$$\left[\frac{(d_1d_4 - d_2d_3)}{(d_1+d_4)^2} - \frac{(d_1+d_2)}{(d_1+d_4)}\right]b^2 + \left[-2h_1\frac{(d_1d_4 - d_2d_3)}{(d_1+d_4)^2} + \frac{h_1}{(d_1+d_4)}(d_1+d_2+d_4) + \frac{d_3au^*}{(d_1+d_4)(u^*+e_1)} - h_1 + \frac{au^*}{u^*+e_1}\right]b + \frac{(d_1d_4 - d_2d_3)}{(d_1+d_4)^2}h_1^2 - \frac{h_1^2d_4}{(d_1+d_4)} - \frac{h_1d_3au^*}{(d_1+d_4)(u^*+e_1)} = 0 \quad (46)$$

and the critical value of bifurcation parameter b is equal to b_T, where

$$b_T = \frac{-B \pm \sqrt{B^2 - 4AC}}{2A} \quad (47)$$

and

$$A = -\frac{d_2d_3 + d_1^2 + d_1d_2 + d_2d_4}{(d_1+d_4)^2},$$
$$B = \frac{h_1}{(d_1+d_4)^2}\left[a\frac{(d_1+d_4)}{1-2u^*-e_1}(d_1+d_3+d_4) + 2d_2d_3 + d_1d_2 - d_1d_4\right],$$
$$C = -\left(\frac{h_1}{d_1+d_4}\right)^2\left[d_4^2 + d_2 + d_3 + \frac{ad_3(d_1+d_4)}{1-2u^*-e_1}\right].$$

Therefore

$$b_T = \frac{h_1\left[a\frac{(d_1+d_4)}{1-2u^*-e_1}(d_1+d_3+d_4) + 2d_2d_3 + d_1d_2 - d_1d_4 + \sqrt{\tau}\right]}{2(d_2d_3 + d_1^2 + d_1d_2 + d_2d_4)}, \quad (48)$$

where

$$\tau = 4d_2^2d_3^2 + d_1^2d_2^2 + d_1^2d_4^2 - 2d_1^2d_2d_4 + 4d_2^2d_3d_1 - 4d_1d_2d_3d_4 + a^2[(d_1^4 + d_3^2d_1^2 + 2d_1^3d_3 + d_4^4d_1^2 + d_1^3d_4 + 2d_1^2d_3d_4 + d_4^2d_1^2 + d_4^2d_3^2 + 2d_1d_3d_4^2 + d_4^6 + 2d_1d_4^3 + 2d_3d_4^3 + 2d_1^3d_4 + 2d_1d_4d_3^2 + 4d_1^2d_4d_3 + 2d_1d_4^5 + 4d_1^2d_4^2 + 4d_1d_3d_4^2)\backslash(1 + 4u^{*2} - 4u^* + e_1^2 - 2e_1 + 4u^*e_1)] + 2(2d_2d_3 + d_1d_2 - d_1d_4) \times (ad_1^2 + ad_1d_3 + 2ad_1d_4 + ad_4d_3 + ad_4^2)\backslash(1 - 2u^* - e_1).$$

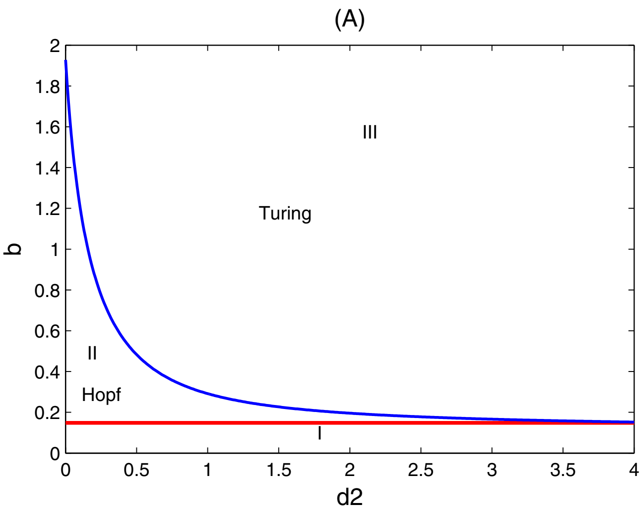

Fig. 1. Bifurcation diagram of model (4) with $a = 0.9$, $e_1 = 0.1$, $e_2 = 0.05$, $d_1 = 0.3$, $d_3 = -0.2$, $d_4 = 0.4$. The red and blue lines correspond to the Hopf b_h and Turing b_T bifurcation critical lines respectively. The figure shows the Turing space (it is marked by III) with the area bounded by the Turing bifurcation line and the Hopf bifurcation line.

Now, we study the dynamical behavior of the spatial predator–prey model (2) via numerical simulation. We check whether a spatially homogeneous equilibrium is stable, unstable and to which solution to converge. For this, we fix the model values and vary d_2 as a function of b. We plot the bifurcation diagram of linear stability analysis in Fig. 1. The bifurcation lines divide the parameter space into three distinct regions. In region I, both Hopf and Turing bifurcations occur. The equilibria that can be found in the area, II, are stable with respect to the homogeneous perturbations but lose their stability to homogeneous perturbations of specific wave number k. The upper regions of the parameter space corresponds to the system with homogeneous unconditionally stable equilibria.

Figure 2 indicates the Turing space properly. We plot the dispersion relation for different values of d_2 and other parameter values are mentioned in the caption of the figure by keeping $b = 0.01$. We find that when d_2 is increased, the available Turing modes $[\mathrm{Re}(\lambda) > 0]$ are decreased and all available modes are weakened.

3.1. *Turing instability*

The positive equilibrium $w_3 = (u^*, v^*)$ has Turing instability if it is asymptotically stable for system (17), but it is unstable with respect to solutions of model (4).

In particular, when system (4) has no diffusion, the characteristic polynomial equation of

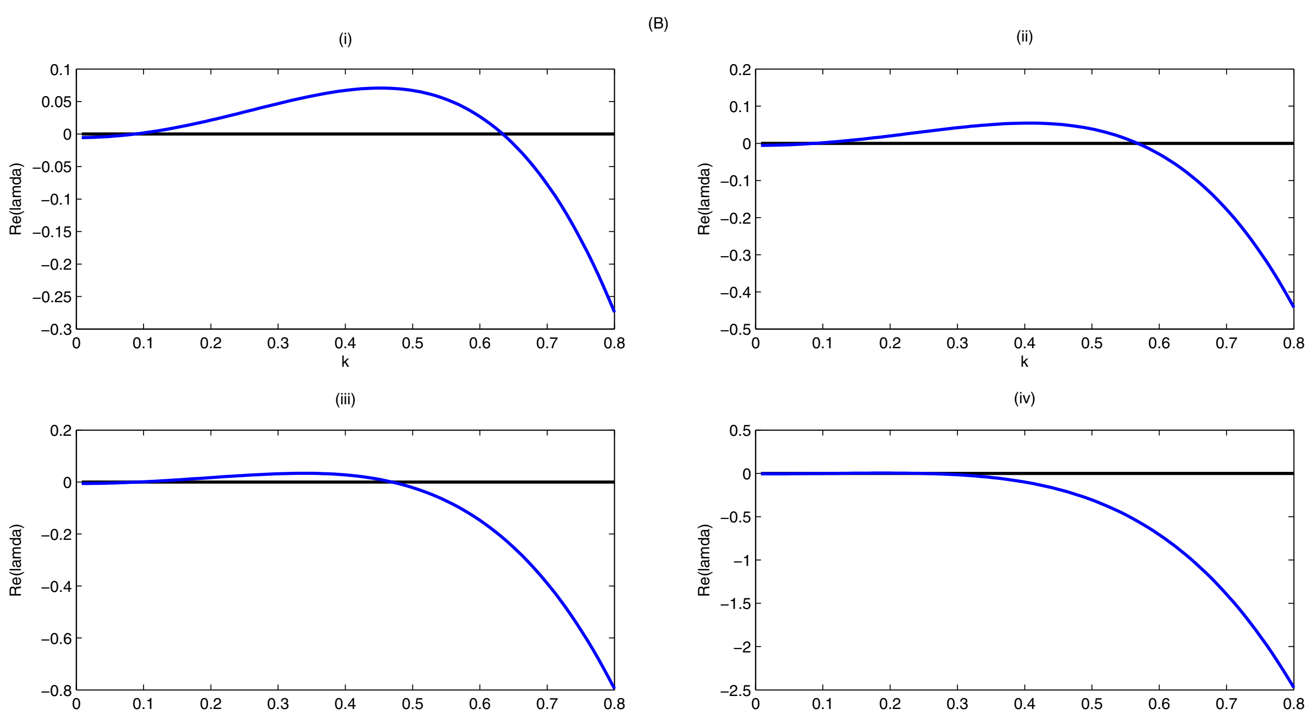

Fig. 2. Variation of dispersion relation of model (4) with the parameter values $a = 0.9$, $e_1 = 0.1$, $e_2 = 0.05$, $d_1 = 0.3$, $d_3 = -0.2$ and $d_4 = 6$. For different values of d_2, (i) $d_2 = 0.1$, (ii) $d_2 = 2$, (iii) $d_2 = 6$ and (iv) $d_2 = 25$.

the ODE system (17) at the positive equilibrium $w^* = (u^*, v^*)$ is

$$\lambda^2 - \lambda(h_1 + h_4) + h_1h_4 - h_2h_3 = 0. \quad (49)$$

It is easy to check that the real parts of λ are negative if

$$2u^* + \frac{e_1(1 - u^*)}{u^* + e_1} > 1. \quad (50)$$

Next we study the Turing instability of system (4).

Case 1 ($d_2 = d_3 = 0$).

Consider (4) without cross-diffusion, then (33) becomes

$$E_k = d_1d_4k^4 - (d_1h_4 + d_4h_1)k^2 + h_1h_4 - h_2h_3. \quad (51)$$

If condition (50) holds, then we have $E_k > 0$ and $H_k < 0$. Thus $\mathrm{Re}(\lambda) < 0$, therefore we deduce the following result by Theorem 5.1.1 in [Henry, 1981].

Proposition 3. *Assume that (50) holds. If $d_2 = d_3 = 0$, then the positive steady state $w^* = (u^*, v^*)$ of (4) is locally asymptotically stable. As a consequence, Turing instability does not occur for problem (4).*

Case 2 ($d_2 \neq 0$ or $d_3 \neq 0$).

Assume (50), that is $w^* = (u^*, v^*)$ is stable for ODE system (17) and suppose $\rho = k^2 \geq 0$ in Eqs. (32) and (33) then we have

$$H_k = H(\rho) = (d_1 + d_4)\rho - (h_1 + h_4) \quad (52)$$

and

$$\begin{aligned} E_k &= E(\rho) \\ &= (d_1d_4 - d_2d_3)\rho^2 - (d_1h_4 + d_4h_1 \\ &\quad - d_2h_3 - d_3h_2)\rho + h_1h_4 - h_2h_3 \\ &= p_1\rho^2 - p_2\rho + p_3. \end{aligned} \quad (53)$$

The Turing instability sets in when at least one of the following conditions is violated:

$$H(\rho) < 0 \quad \text{and} \quad E(\rho) > 0. \quad (54)$$

If the condition $h_1 + h_4 < 0$ is met, it is clear that the first condition $H(\rho) < 0$ is not violated. Hence the condition $E(\rho) > 0$ gives rise to diffusion-driven instability.

Thus, a necessary condition for $w^* = (u^*, v^*)$ of (4) becomes unstable when

$$E(\rho) = p_1\rho^2 - p_2\rho + p_3 < 0. \quad (55)$$

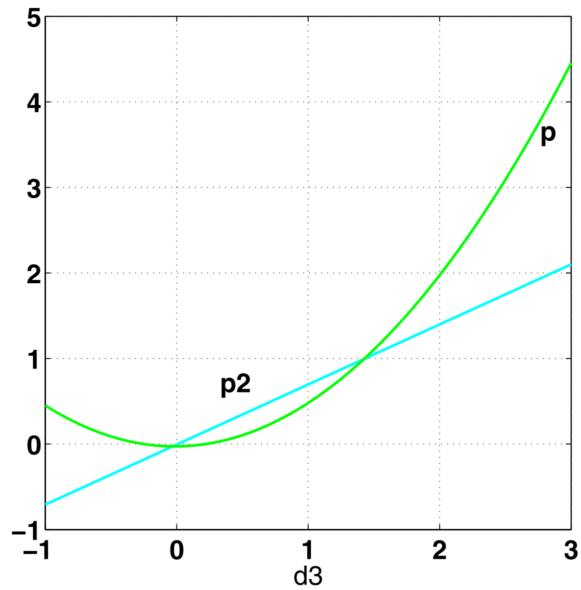

Fig. 3. Emergence of Turing pattern corresponding to $p_2 = ((d_1h_4 + d_4h_1) - (d_2h_3 + d_3h_2))$, $p = ((d_1h_4 + d_4h_1) - (d_2h_3 + d_3h_2))^2 - 4(h_1h_4 - h_2h_3) * (d_1d_4 - d_2d_3)$.

For that, we need $p_2 > 0$ and $p_2^2 - 4p_1p_3 > 0$ for some ρ.

The equation $p_1\rho^2 - p_2\rho + p_3 = 0$, has two positive roots $\rho_1 = \frac{p_2 - \sqrt{p_2^2 - 4p_1p_3}}{2p_1}$ and $\rho_2 = \frac{p_2 - \sqrt{p_2^2 + 4p_1p_3}}{2p_1}$.

It is clear that if $\rho_1 < \rho < \rho_2$, then the condition (55) is satisfied and these results are summarized in the following proposition.

Proposition 4. *Assume that (50) holds and*

$$p_2 > 0, \quad p_2^2 - 4p_1p_3 > 0. \quad (56)$$

Then the positive steady state $w^* = (u^*, v^*)$ of (4) is unstable and so (4) has Turing instability provided that $\rho_1 < \rho < \rho_2$.

Remark 3.1. Under the assumption (50)

(i) When $d_3 = 0$ and $d_2 \neq 0$ we obtain $p_2 < 0$ and there is no Turing instability.
(ii) When $d_2 = 0$, $d_3 \neq 0$ or $d_2d_3 \neq 0$. If $\frac{au^*}{u^* + e_1} > 0$, then $p_2 > 0$ and $p_2^2 - 4p_1p_3 > 0$ when d_3 is large enough. If there exists some ρ such that $\rho_1 < \rho < \rho_2$, Turing instability can emerge if the cross-diffusion coefficient d_3 is large enough.

4. Pattern Formation

In this section, we perform numerical simulations of model (4) in two-dimensional (2D) space, in order

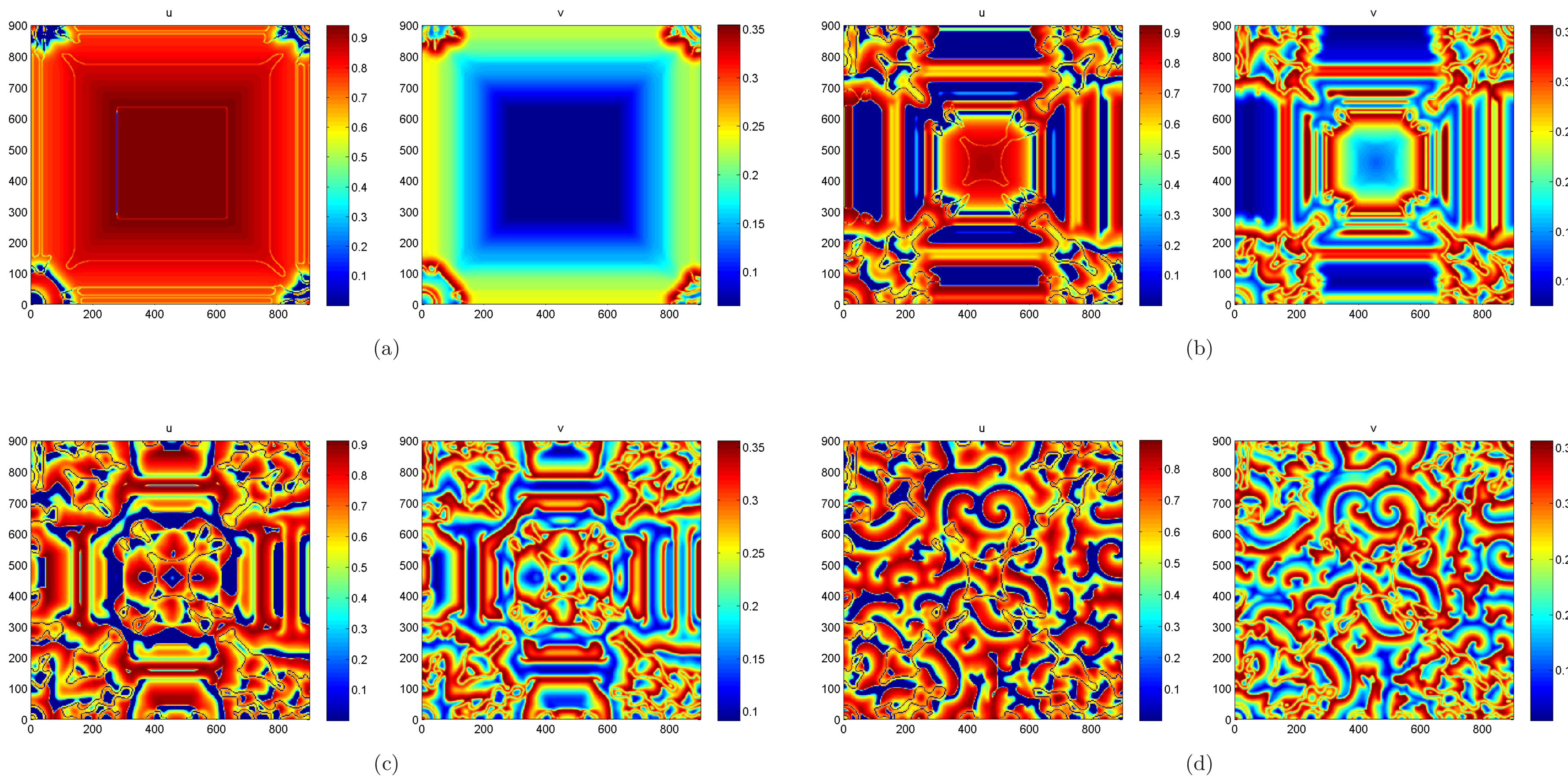

Fig. 4. Snapshots of contour of the time evolution of the prey and predator at different instants, (a) $t = 1000$, (b) $t = 1800$, (c) $t = 3000$ and (d) $t = 20\,000$.

to show the evolution of the spatial pattern of prey and predator in the time evolution and effect of cross-diffusion for pattern formation. Our numerical simulations use the zero-flux boundary conditions (4) with a system size of 900 × 900 by using finite-difference methods.

The initial condition is a small perturbation in the vicinity of equilibrium point (u^*, v^*) and we consider the following parameter values:

$$\begin{gathered} a = 0.9, \quad b = 0.01, \quad e_1 = 0.1, \quad e_2 = 0.05, \\ d_1 = 0.3, \quad d_3 = -0.2, \quad d_4 = 0.4. \end{gathered} \tag{57}$$

The left figures are the evolution of the prey spatial distribution and the right figures are the predators'. Figure 4 shows the evolution of the spatial patterns of the prey and the predator for different values of time and $d_2 = 0.1$. In this case, we observe that for system (4) the random initial distribution leads to the formation of irregular patterns. As the time is increased, the dynamics of the system does not undergo any further changes.

Next, we study the effect of the cross-diffusion d_2 on the predator–prey model. We plot the evolution of the spatial pattern for a fixed time and for different values of d_2.

For $d_2 = 0.1$, Fig. 5(a) [resp., Fig. 6(a)] shows the evolution of the spatial pattern of the prey (resp., of the predator) at $t = 20\,000$. We conclude from these figures that the labyrinth patterns prevail in the whole domain.

Figure 5(b) [resp., Fig. 6(b)] shows the evolution of the spatial pattern of the prey (resp., of the

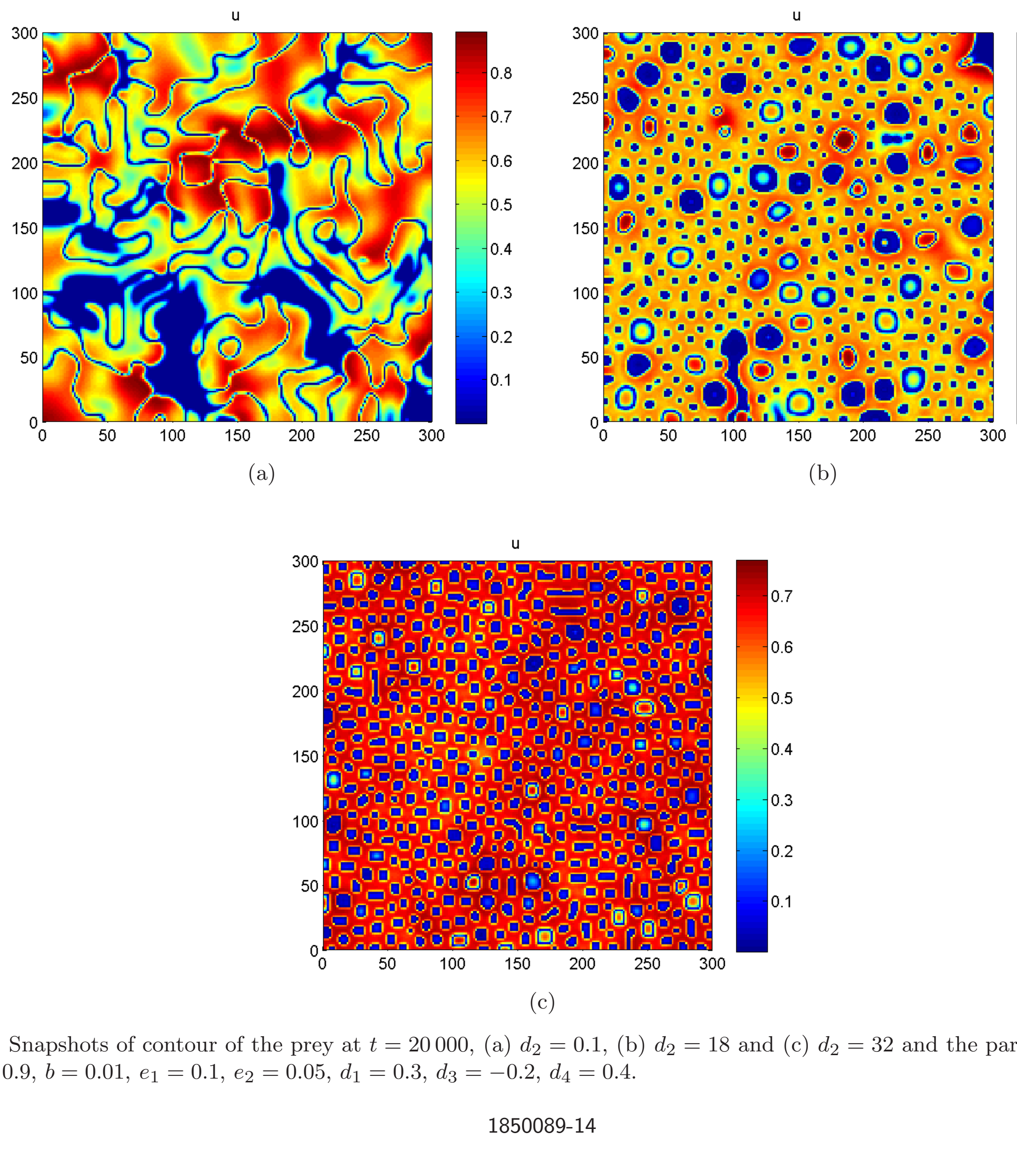

Fig. 5. Snapshots of contour of the prey at $t = 20\,000$, (a) $d_2 = 0.1$, (b) $d_2 = 18$ and (c) $d_2 = 32$ and the parameters values are $a = 0.9$, $b = 0.01$, $e_1 = 0.1$, $e_2 = 0.05$, $d_1 = 0.3$, $d_3 = -0.2$, $d_4 = 0.4$.

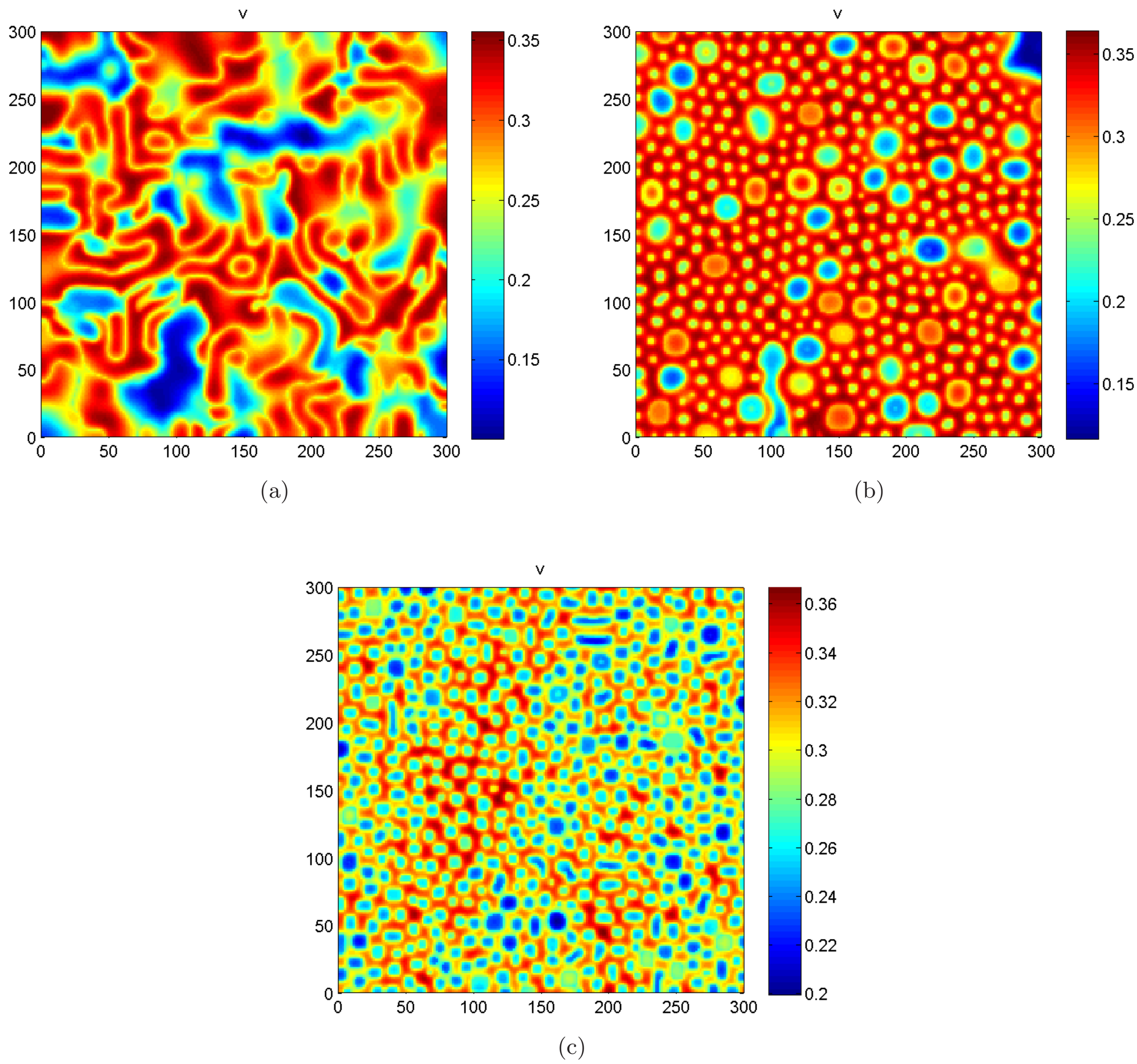

Fig. 6. Snapshots of contour of the predator at $t = 20\,000$, (a) $d_2 = 0.1$, (b) $d_2 = 18$ and (c) $d_2 = 32$ and the parameter values are $a = 0.9$, $b = 0.01$, $e_1 = 0.1$, $e_2 = 0.05$, $d_1 = 0.3$, $d_3 = -0.2$, $d_4 = 0.4$.

predator) at $t = 20\,000$ and for $d_2 = 18$. We conclude from these figures that the spots and labyrinth mixture patterns prevail in the entire field.

As d_2 increases to 32, we plot the evolution of the spatial pattern of the prey (resp., of the predator) at $t = 20\,000$, see Fig. 5(c) [resp., Fig. 6(c)], We conclude from these figures, the spotted spatial patterns over the whole domain.

5. Conclusion

This work presents the spatiotemporal dynamics of a predator–prey model of Holling-type II functional response and the effect of cross-diffusion. We have obtained the existence of positive equilibriums and their local stability. By constructing a Lyapunov function, we prove sufficient conditions for global stability of the positive equilibrium. By using suitable numerical simulations, Fig. 1 gives three domains for three kinds of patterns of model (4) and we find that cross-diffusion may induce Turing instability, Hopf instability and Turing–Hopf instability. We found from Fig. 4 that reaction–diffusion model (4) shows a more complex pattern formation, chaotic wave pattern, which is created by Turing–Hopf instability. The complexity of the pattern formation is induced by the cross-diffusion effect.

If the values of predator cross-diffusion coefficient d_2 is increased, we found that pure Turing instability (Figs. 5 and 6) gives rise to the spotted, striped and labyrinth patterns. These results indicate that the effect of the cross-diffusion for pattern formation in an ecosystem is remarkable.

In [Camara & Aziz-Alaoui, 2008a], the authors studied this predator–prey model only with diffusion, they found that the model only had labyrinth pattern. However, in the present paper, we obtained stripes, spots and labyrinth patterns by using bifurcation theory, thus when d_2 increased so did the spotted spatial patterns over the whole domain. Our results confirm that cross-diffusion can create stationary patterns. For the evolution of the prey–predator spatial distribution, after a while, the behavior becomes more complex against results in [Camara & Aziz-Alaoui, 2008a]. The results well enriched the findings in Holling–Tanner predator–prey models.

References

Abid, W., Yafia, R., Aziz-Alaoui, M. A., Bouhafa, H. & Abichou, A. [2015a] "Instability and pattern formation in three-species food chain model via Holling-type II functional response on a circular domain," *Int. J. Bifurcation and Chaos* **25**, 1550092-1–25.

Abid, W., Yafia, R., Aziz-Alaoui, M. A., Bouhafa, H. & Abichou, A. [2015b] "Global dynamics on a circular domain of a diffusion predator–prey model with modified Leslie–Gower and Beddington–DeAngelis functional type," *Evol. Eqs. Contr. Th.* **4**, 115–129.

Abid, W., Yafia, R., Aziz-Alaoui, M. A., Bouhafa, H. & Abichou, A. [2015c] "Diffusion driven instability and Hopf bifurcation in spatial predator–prey model on a circular domain," *Appl. Math. Comput.* **260**, 292–313.

Arditi, R. & Ginzburg, L. R. [1989] "Coupling in predator–prey dynamics: Ratio-dependence," *J. Theoret. Biol.* **139**, 311–326.

Aziz-Alaoui, M. A. & Daher Okiye, M. [2003] "Boundedness and global stability for a predator–prey model with modified Leslie–Gower and Holling-type II schemes," *Appl. Math. Lett.* **16**, 1069–1075.

Camara, B. I. & Aziz-Alaoui, M. A. [2008a] "Dynamics of predator–prey model with diffusion," *Dyn. Contin. Discr. Impuls. Syst. Ser. A* **15**, 897–906.

Camara, B. I. & Aziz-Alaoui, M. A. [2008b] "Turing and Hopf patterns formation in a predator–prey model with Leslie–Gower type functional response," *Dyn. Contin. Discr. Impuls. Syst. Ser. B* **16**, 897–906.

Chattopadhyay, J., Sarkar, A. K. & Tapaswi, P. K. [1996] "Effect of cross-diffusion on a diffusive prey–predator system a nonlinear analysis," *J. Biol. Syst.* **4**, 159–169.

Chung, J. & Peacock-López, E. [2007] "Bifurcation diagrams and Turing patterns in a chemical self-replicating reaction–diffusion system with cross diffusion," *Chem. Phys.* **127**, 174903.

Daher Okiye, M. & Aziz-Alaoui, M. A. [2002] "On the dynamics of a predator–prey model with the Holling–Tanner functional," *Proc. ESMTB Conf.*, ed. Capasso, V., pp. 270–278.

Dancer, E. N. [1984] "On positive solutions of some pairs of differential equations," *Trans. Amer. Math. Soc.* **284**, 729–743.

DeAngelis, D. L., Goldstein, R. A. & O'Neill, R. V. [1975] "A model for trophic interaction," *Ecology* **56**, 881–892.

Dubey, B. & Das, B. [2001] "A predator–prey interaction model with self and cross-diffusion," *Ecol. Model.* **141**, 67–76.

Freedman, H. I. [1987] *Deterministic Mathematical Models in Population Ecology* (HIFR Consulting Ltd., Edmonton).

Henry, D. [1981] *Geometric Theory of Semilinear Parabolic Equations*, Lecture Notes in Mathematics, Vol. 840 (Springer-Verlag).

Holling, C. S. [1959] "The components of predation as revealed by a study of small mammal predation of the European pine sawfly," *Canad. Entomol.* **91**, 293–320.

Hsu, S. B. & Hwang, T. W. [1999] "Hopf bifurcation analysis for a predator–prey system of Holling and Leslie type," *Taiwanese J. Math.* **3**, 35–53.

Hu, G.-P. & Li, X.-L. [2012] "Turing patterns of a predator–prey model with a modified Leslie–Gower term and cross diffusions," *Int. J. Biomath.* **5**, 203–219.

Jin, Z., Liu, Q.-X. & Li, L. [2008] "Pattern formation induced by cross-diffusion in a predator–prey system," *Chin. Phys. B* **17**, 3936–3941.

Kerner, E. H. [1959] "Further considerations on the statistical mechanics of biological associations," *Bull. Math. Biophys.* **21**, 217–255.

Kuto, K. [2004] "Stability of steady-state solutions to a prey–predator system with cross-diffusion," *J. Diff. Eqs.* **197**, 293–314.

Kuto, K. & Yamada, Y. [2005] "Coexistence states for a prey–predator model with cross-diffusion," *Discrete and Continuous Dynamical Systems*, pp. 536–545.

Leslie, P. [1948] "Some further notes on the use of matrices in population mathematics," *Biometrika* **35**, 213–245.

Li, Y. & Xiao, D. [2007] "Bifurcations of a predator–prey system of Holling and Leslie types," *Chaos Solit. Fract.* **34**, 606–620.

Li, C. [2013] "Global existence of solutions to a cross-diffusion predator–prey system with Holling-type-II functional response," *Comput. Math. Appl.* **65**, 1152–1162.

Lian, X. & Huang, L. [2014] "Simulation of pattern in a cross-diffusive predator–prey system with the Allee effect," *J. Inform. Comput. Sci.* **11**, 527–534.

Liang, Z. & Pan, H. [2007] "Qualitative analysis of a ratio-dependent Holling–Tanner model," *J. Math. Anal. Appl.* **334**, 954–964.

Lotka, A. J. [1925] *Elements of Physical Biology* (Williams and Wilkins, Baltimore).

Murray, J. D. [1993] *Mathematical Biology* (Springer-Verlag, Berlin).

Nindjin, A. F., Aziz-Alaoui, M. A. & Cadivel, M. [2006] "Analysis of a predator–prey model with modified Leslie–Gower and Holling-type II schemes with time delay," *Nonlin. Anal.: Real World Appl.* **7**, 1104–1118.

Okubo, A. [1980] *Diffusion and Ecological Problems: Mathematical Models*, Biomathematics, Vol. 10 (Springer, Berlin).

Rosen, G. [1977] "Effects of diffusion on the stability of the equilibrium in multi-species ecological systems," *Bull. Math. Biol.* **39**, 373–383.

Shi, J., Xie, Z. & Little, K. [2011] "Cross-diffusion induced instability and stability in reaction–diffusion systems," *J. Appl. Anal. Comput.* **1**, 95–119.

Shigesada, N., Kawasaki, K. & Teramoto, E. [1979] "Spatial segregation of interacting species," *J. Theor. Biol.* **79**, 83–99.

Sun, X.-K., Huo, H.-F. & Xiang, H. [2009] "Bifurcation and stability analysis in predator–prey model with a stage-structure for predator," *Nonlin. Dyn.* **58**, 497–513.

Sun, G.-Q., Jin, Z., Li, L., Haque, M. & Li, B.-L. [2012] "Spatial patterns of a predator–prey model with cross-diffusion," *Nonlin. Dyn.* **69**, 1631–1638.

Turing, A. M. [1952] "The chemical basis of morphogenesis," *Philos. Trans. Roy. Soc. B* **237**, 37–72.

Volterra, V. [1926] "Variazioni e fluttuazioni del numero d'individui in specie d'animali conviventi," *Mem. Acad. Lincei* **2**, 31–113.

Wang, M. [2008] "Stability and Hopf bifurcation for a prey–predator model with prey-stage structure and diffusion," *Math. Biosci.* **212**, 149–160.

Wang, W.-M., Wang, W.-J., Lin, Y.-Z. & Tan, Y.-J. [2011] "Pattern selection in a predation model with self and cross-diffusion," *Chin. Phys. B* **20**, 034702.

Wen, Z. [2013] "Turing instability and stationary patterns in a predator–prey systems with nonlinear cross-diffusions," *Wen Boundary Value Problems*, 10.1186/1687-2770-2013-155.

Xu, S. [2008] "Existence of global solutions for predator–prey model with cross-diffusion," *Electron. J. Diff. Eqs.* **06**, 1–14.

Yafia, R. & Aziz-Alaoui, M. A. [2013] "Existence of periodic travelling waves solutions in predator–prey model with diffusion," *Appl. Math. Model.* **37**, 3635–3644.

Zhou, J. & Kim, C.-G. [2013] "Positive solutions for a Lotka–Volterra prey–predator model with cross-diffusion and Holling-type-II functional response," *Sci. China — Math.* **57**, 991–1010.